


Article

Multi-Objective Optimization for Mixed-Model Two-Sided Disassembly Line Balancing Problem Considering Partial Destructive Mode

Bao Chao ¹, Peng Liang ¹, Chaoyong Zhang ^{1,*} and Hongfei Guo ^{2,*}¹ The State Key Laboratory of Digital Manufacturing Equipment and Technology, Huazhong University of Science and Technology, Wuhan 430074, China² School of Intelligent Systems Science and Engineering, Jinan University, Zhuhai 519070, China

* Correspondence: zcyhust@hust.edu.cn (C.Z.); ghf_2005@jnu.edu.cn (H.G.)

Abstract: Large-volume waste products, such as refrigerators and automobiles, not only consume resources but also pollute the environment easily. A two-sided disassembly line is the most effective method to deal with large-volume waste products. How to reduce disassembly costs while increasing profit has emerged as an important and challenging research topic. Existing studies ignore the diversity of waste products as well as uncertain factors such as corrosion and deformation of parts, which is inconsistent with the actual disassembly scenario. In this paper, a partial destructive mode is introduced into the mixed-model two-sided disassembly line balancing problem, and the mathematical model of the problem is established. The model seeks to comprehensively optimize the number of workstations, the smoothness index, and the profit. In order to obtain a high-quality disassembly scheme, an improved non-dominated sorting genetic algorithm-II (NSGA-II) is proposed. The proposed model and algorithm are then applied to an automobile disassembly line as an engineering illustration. The disassembly scheme analysis demonstrates that the partial destructive mode can raise the profit of a mixed-model two-sided disassembly line. This research has significant application potential in the recycling of large-volume products.

Keywords: multi-objective; mixed-model; two-sided; disassembly line balancing; partial destructive mode

MSC: 90B30



Citation: Chao, B.; Liang, P.; Zhang, C.; Guo, H. Multi-Objective Optimization for Mixed-Model Two-Sided Disassembly Line Balancing Problem Considering Partial Destructive Mode.

Mathematics **2023**, *11*, 1299. <https://doi.org/10.3390/math11061299>

Academic Editor: Andrea Scozzari

Received: 30 December 2022

Revised: 30 January 2023

Accepted: 6 February 2023

Published: 8 March 2023



Copyright: © 2023 by the authors. Licensee MDPI, Basel, Switzerland. This article is an open access article distributed under the terms and conditions of the Creative Commons Attribution (CC BY) license (<https://creativecommons.org/licenses/by/4.0/>).

1. Introduction

The lifecycle of products is continually getting shorter due to the quick development of new technology and advances in science. Many products are quickly phased out due to outdated functions, or scrapped, leading to the generation of more and more waste [1]. Remanufacturing is the manufacturing of waste products as raw materials, which can effectively conserve energy and resources and significantly lowers production costs. Disassembly is the first and mandatory step of remanufacturing; it plays a significant role in recycling of resources [2–4].

Paced assembly lines are increasingly being used by recycling companies instead of the fixed disassembly position layout. They have a great advantage in efficiency while dealing with a significant volume of waste products. In the process of disassembly, the priorities among parts must be taken into consideration and the toxic residues must be removed. How to rationally assign the tasks to the stations on the paced line to achieve the optimal goals under these constraints is called the disassembly line balancing problem (DLBP), which was first proposed by Gupta and Gungor [5] and has garnered considerable interest from experts and scholars from related fields.

According to the different objectives and conditions, DLBPs mainly fall into two major types. As addressed in our study, the type of DLBP that aims to minimize the number

of workstations for a given cycle time is called DLBP-I. DLBP- II has the objective of minimizing the cycle time with a fixed number of workstations. The majority of DLBP research is focused on Type-I, and based on this, the optimization aims are expanded to include additional factors to make it more practical for disassembly businesses. The following are some of the most commonly considered objectives: energy consumption [6,7], workload smoothness index [8], number of workers [9], disassembly profit [7], and line efficiency [10].

Complete disassembly necessitates the removal of every part, whereas partial disassembly only necessitates the removal of required and hazardous parts, leaving the remaining parts intact [11]. It is obvious that for disassembling businesses, the partial disassembly mode is more suited to lowering costs and raising productivity and profits. In addition to this, unlike assembly lines, disassembly lines are facing uncertainty factors, such as corrosion and deformation of the connectors, which makes it difficult for each part to be removed conventionally [12,13]. At the same time, the conventional disassembly mode is not suitable for the disassembling of low-value and long task time parts. Pointing to this condition, a partial destructive disassembly mode is considered in this article [7]. In this mode, the major parts of the waste products are conventionally disassembled, and the rest of the parts are destructively disassembled or discarded under cost considerations.

Single-model disassembly lines are designed to produce high volumes of standardized homogeneous products, making them unsuitable for customer demand with a wide range of products. Firms tend to add a new disassembly line for new waste product during the recycling process. This strategy has drawbacks such as higher disassembly costs, wasted layout space, and decreased disassembly efficiency. A more cost-effective alternative for the disassembly of waste products with comparable assembly structures is to achieve mixed disassembly of these products on the same disassembly line [14]. When disassembling on two-sided lines, the disassembly tasks could be distinct because of variations in part designs, or the disassembly of the same part might result in different operating times and value because of variations in waste products' quality [15]. There are few studies on the mixed model two-sided disassembling line problem, and the existing studies lack the consideration of the uncertainty of the product state and how to maximize the disassembly revenue through partial destructive disassembly.

It was proved that DLBP is an NP-complete problem [16]. Since the problem was proposed, various methods have been developed to solve it. Exact methods primarily use integer programming and dynamic programming to solve the DLBP in solvers, such as CPLEX, LINGO, and GUROBI [17,18]. With increasing DLBP scale, exact methods are unable to provide feasible disassembly solutions in a reasonable time, so heuristic and metaheuristic methods are proposed [19]. For heuristics, the AHP with PROMETHEE [20] and a greedy/2-opt algorithms [21] are mainly applied. For meta-heuristics, this includes traditional algorithms like genetic, simulated annealing, ant colony, artificial bee colony, etc., [22–24] and recently, other algorithms have been proposed, such as gravitational search, gray wolf, migrating birds optimization, etc. [25,26]. According to the findings, meta-heuristics are more computationally efficient than the other two types of approaches, and they can lead to satisfactory answers [27].

Although the existing literature has made great progress in the research of DLBP, there are still gaps in the following aspects: Above all, the current research on the mixed-model two-sided disassembly of large-volume waste products did not take into account the partial destructive mode and the tool changes during the disassembly process. Secondly, existing studies only focus on single objectives such as profit maximization or workstation minimization as optimization goals, without comprehensive consideration of various needs of enterprises. In the end, there is a lack of a feasible case to provide research for this type of problem.

In view of the shortcomings of the current research, this paper takes minimizing the number of workstations, minimizing the smoothness index, and maximizing the profit as the objectives, and studies the mixed-model two-sided disassembly line balancing problem

suitable for large-volume waste products disassembling in the partial destructive mode. The main contributions can be listed as follows. Firstly, a new multi-objective mathematical model is developed for solving PD-MTDLBP. Secondly, an improved NSGA-II algorithm is proposed for multi-objective optimisation of PD-MTDLBP. Finally, a multi-model case transformed from a real disassembly scenario is provided.

The remainder of this paper is structured as follows. In Section 2, the partial destructive mixed-model two-sided disassembly line balancing problem (PD-MTDLBP) is described, and the MIP formulation of PD-MTDLBP is presented. In Section 3, the proposed approach for solving PD-MTDLBP is given in detail. In Section 4, a computational example to validate the performance of the proposed model and algorithm are given. Conclusions are then drawn in the final section, along with suggestions for further research avenues.

2. Problem Statement

2.1. Problem Description

In the arrangement of a two-sided disassembly line, the workstations are symmetrically positioned along both sides of the conveyor. The stations on the left and right sides refer to one another as a companion station. Together, they form a mated station. Each workstation has a corresponding operator and disassembly tools [28]. The disassembly task is subject to the disassembly direction constraint on the two-sided disassembly line, which can be divided into three types: left type (L), right type (R), and either type (E). Each type of task is only allowed to be disassembled in its corresponding direction.

A two-sided disassembly line is referred to as a mixed-model two-sided disassembly line if it is used to disassemble multiple waste products with similar structural characteristics in a mixed flow [29]. Each waste product has a task disassembly precedence relationship that can be combined to create a joint disassembly precedence diagram.

Generally speaking, destructive disassembly can increase the efficiency of disassembly, thereby lowering energy consumption and disassembly costs, but it can also make parts less valuable. Hence, parts that are not in high demand or not hazardous can be disassembled either conventionally or destructively. High-demand and hazardous parts, on the other hand, must be disassembled conventionally.

2.2. Mathematical Model

The mathematical model for PD-MTDLBP is as follows, and the parameters and variables required by the model are as shown in Appendix A.

$$\min f_1 = \sum_{s \in S} \sum_{k=1,2} W_{sk} \quad (1)$$

$$\min f_2 = \sqrt{\sum_{s \in S} \sum_{k=1,2} (T_{sk} - \max\{T_{sk}\})^2 / \sum_{s \in S} \sum_{k=1,2} W_{sk}} \quad (2)$$

$$\begin{aligned} \max f_3 = & \sum_{i \in I} \sum_{e=1,2} x_i v_{ie} - \sum_{m \in M} \sum_{i \in I} \sum_{s \in S} \sum_{k=1,2} \sum_{e=1,2} (x_{isk} c_{ie} + x_{isk} t_{ie}^m (c_s + h_i c_h)) \\ & - \sum_{s \in S} \sum_{k=1,2} \sum_{q \in Q} \sum_{i \in I} \sum_{j \in I} x_{iskq} x_{jsk(q+1)} z_{ij} t_t c_s - |S| c_f \end{aligned} \quad (3)$$

s.t.

$$x_i = 1, \forall i \in \{i | h_i^m + d_i^m \geq 1\} \quad (4)$$

$$x_i \leq 1, \forall i \in \{i | h_i^m + d_i^m = 0\} \quad (5)$$

$$x_j = 1, \forall P_{ij} = 1, x_i = 1 \quad (6)$$

$$x_i e_i = 1, \forall i \in \{i | h_i^m + d_i^m \geq 1\} \quad (7)$$

$$e_i \leq 1, \forall i \in \{i | (h_i^m + d_i^m = 0) \wedge (x_i = 1)\} \quad (8)$$

$$\sum_{s \in S} \sum_{k=1,2} x_{isk} = 1, \forall i \in \{i | x_i = 1\} \quad (9)$$

$$\sum_{m \in M} \sum_{i \in I} \sum_{e=1,2} x_{isk} t_{ie}^m + \sum_{k=1,2} \sum_{q \in Q} \sum_{i \in I} \sum_{j \in I} x_{iskq} x_{jsk(q+1)} z_{ij}^t t_t \leq CT, \forall s \in S, k \in \{1,2\} \quad (10)$$

$$\sum_{s' \in S} \sum_{k \in K(j)} s' x_{js'k} \leq \sum_{s \in S} \sum_{k \in K(i)} s x_{isk}, \forall P_{ij} = 1, x_i x_j = 1 \quad (11)$$

$$\sum_{i \in I} y_{ibs} t_{ie}^m \geq \sum_{j \in I} y_{jas} t_{je}^m + \sum_{k \in K(a)} x_{ask} t_{ae}^m, \forall P_{ba} = 1, m \in M, s \in S, x_b x_a = 1 \quad (12)$$

$$\sum_{k=1,2} x_{isk} + \sum_{k=1,2} x_{jsk} \leq 1 + (y_{ijs} + y_{jis}), \forall ij \in I, s \in S \quad (13)$$

$$\sum_{i \in I} x_{isk} \leq n W_{sk}, \forall s \in S, k = 1,2 \quad (14)$$

$$\sum_{k=1,2} W_{sk} - 2G_s - F_s = 0, \forall s \in S \quad (15)$$

$$G_s \leq G_{s-1}, \forall s \in \{2, \dots, |S|\} \quad (16)$$

In the objective functions, the number of workstations is minimized by Equation (1). Workloads on of the disassembly line are smoothed by Equation (2). Disassembly profit is maximized by Equation (3) [30]. In the constraints, Equations (4) and (5) represents that the parts that are hazardous or demanded must be disassembled; the rest of the parts are disassembled randomly [7]. All of a task's immediate predecessors must be completed in order for it to be performed, as shown in Equation (6). Equations (7) and (8) indicate that the parts that are hazardous or demanded must be disassembled in conventional mode, whilst others can be disassembled in destructive or conventional mode. Equation (9) denotes that the parts selected for disassembly must be assigned to a workstation. Equation (10) represents the cycle time constraint. For the whole disassembly line, the mated-station index of the immediate predecessor must not be greater than that of the immediate successor, as shown in Equation (11). Equation (12) represents the precedence constraint of tasks within the same workstation. Equation (13) represents the position constraint within the station, which defines the relative position between two tasks successively assigned to the same workstation. Equation (14) is the disassembly station and disassembly task constraint, so that the workstation is opened after the disassembly task is assigned. Equation (15) indicates that the total number of workstations is equal to the sum of the mated stations and companion stations [31]. Formula (16) indicates that the mated stations are started one by one.

3. The Proposed Method

For the purpose of solving multi-objective optimisation problems (MOP), meta-heuristic algorithms have been repeatedly shown to be very efficient. In this study, the non-dominated sorting genetic algorithm-II (NSGA-II) is improved and applied to address the proposed PD-MTDLBP. The NSGA-II algorithm is a Pareto-based approach, and its optimal solution set is essentially the non-inferior solution to the MOP. The NSGA algorithm is improved from the following aspects. Based on the multi-chromosomes encoding method proposed by Wang [7] et al., a decoding method suitable for PD-DLBP was constructed. Two processes, two-point crossover and single-point mutation, suitable for multi-chromosomes operations, are applied to generate new populations. The NSGA-II flowchart is depicted in Figure 1, and the detailed processes are given below.

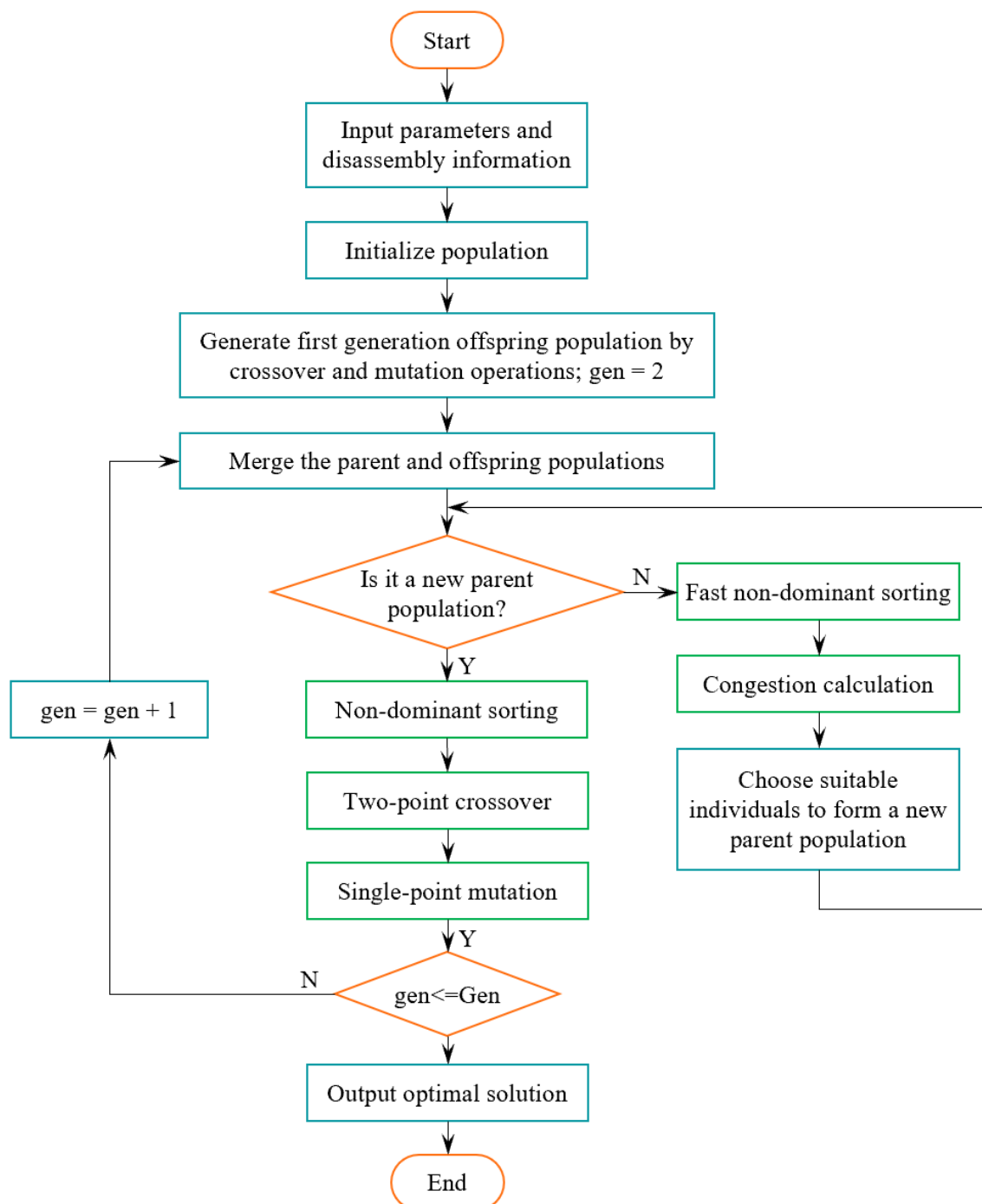


Figure 1. Flowchart of NSGA-II.

3.1. Encoding

Encoding, also known as the process of coming up with a workable disassembly task sequence, is the first and most important step in solving the PD-MTDLBP problem. Three integer vectors are employed for the encoding of the PD-MTDLBP based on the disassembly precedence matrix: the task sequence vector (TS), task decision vector (TD), and task mode vector (TM). Each vector is a one-dimensional array with N_t elements. The TS designates the order in which the tasks of the mix-model are carried out on the two-sided disassembly line.

The TD determines whether the tasks in the TS participate in the disassembly process, and its encoding process should meet Equations (4)–(6). The TM determines which mode

the tasks involved in the disassembly should adopt. Its encoding process needs to satisfy Equations (7) and (8). Taking Figure 2, as an example, assuming that the hazard index of tasks 4 and 6 is 1, and is 0 for the others; and the demand index of task 2 and 11 is 1, and is 0 for the others. The TS, TD, and TM of a feasible initial solution can be constructed as shown in Table 1.

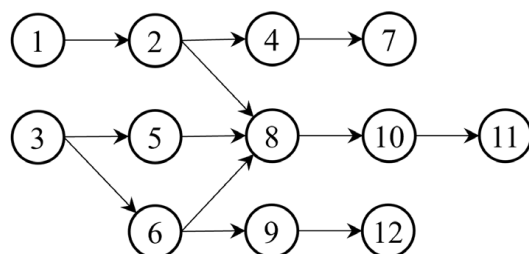


Figure 2. Disassembly precedence diagram.

Table 1. Encoding vector.

Task	1	2	3	4	5	6	7	8	9	10	11	12
TS	3	5	6	9	12	1	2	8	10	4	7	11
TD	1	1	1	0	1	0	1	1	1	1	0	1
TM	1	0	1	-	1	-	1	0	1	1	-	1

3.2. Decoding

During the decoding process, tasks are assigned to each workstation in the order specified in the task sequence vector, subject to cycle time and disassembly direction constraints. The decoding processes are as follows:

Step 1: Turn on the first mated station and begin decoding.

Step 2: Determine whether each model's mated station has received all of the tasks in the TS. Proceed to step 8 if so. If not, move on to step 3.

Step 3: Assign the first task i in the TS as the active task.

Step 4: If $TD[i] = 1$, proceed to step 5. Otherwise, remove current task from TS and return to step 2.

Step 5: Determine the disassembly time of the current task according to $TM[i]$. If there is a tool change, add the required time to the disassembly time.

Step 6: Assign the current task to the left or right side of the mated station if it has a definite disassembly direction (L or R). If E, place it on the side where there is more time for disassembly.

Step 7: If the cycle time constraint is met, assign the task to the current companion station, otherwise, assign the task to a new one. After the assignment, remove the current task from TS and go back to step 2.

Step 8: Output the decoding result.

3.3. Crossover

The crossover of the task sequence vector is usually carried out at random in numerous research. It is easy to produce infeasible individuals by this type of crossing. In this study, a two-point crossover operator is adopted to guarantee that the crossed individuals meet the precedence constraints.

The individuals TS_1 and TS_2 are used to designate two parents of the two-point crossover operation, as seen in Figure 3. Two crossover points P_1 and P_2 are randomly selected in the parent individuals to determine the section of crossover. Keep the sequences before P_1 and after P_2 in TS_1 unchanged. The sub-sequence {9, 12, 1, 2, 8, 10} between P_1 and P_2 in TS_1 becomes {1, 2, 9, 8, 12, 10} through mapping of the same sequence in TS_2 , namely, the offspring individual $N_1 = \{3, 5, 6, 1, 2, 9, 8, 12, 10, 4, 7, 11\}$. Under these crossover operations, the offspring always satisfy the precedence constraint [32].

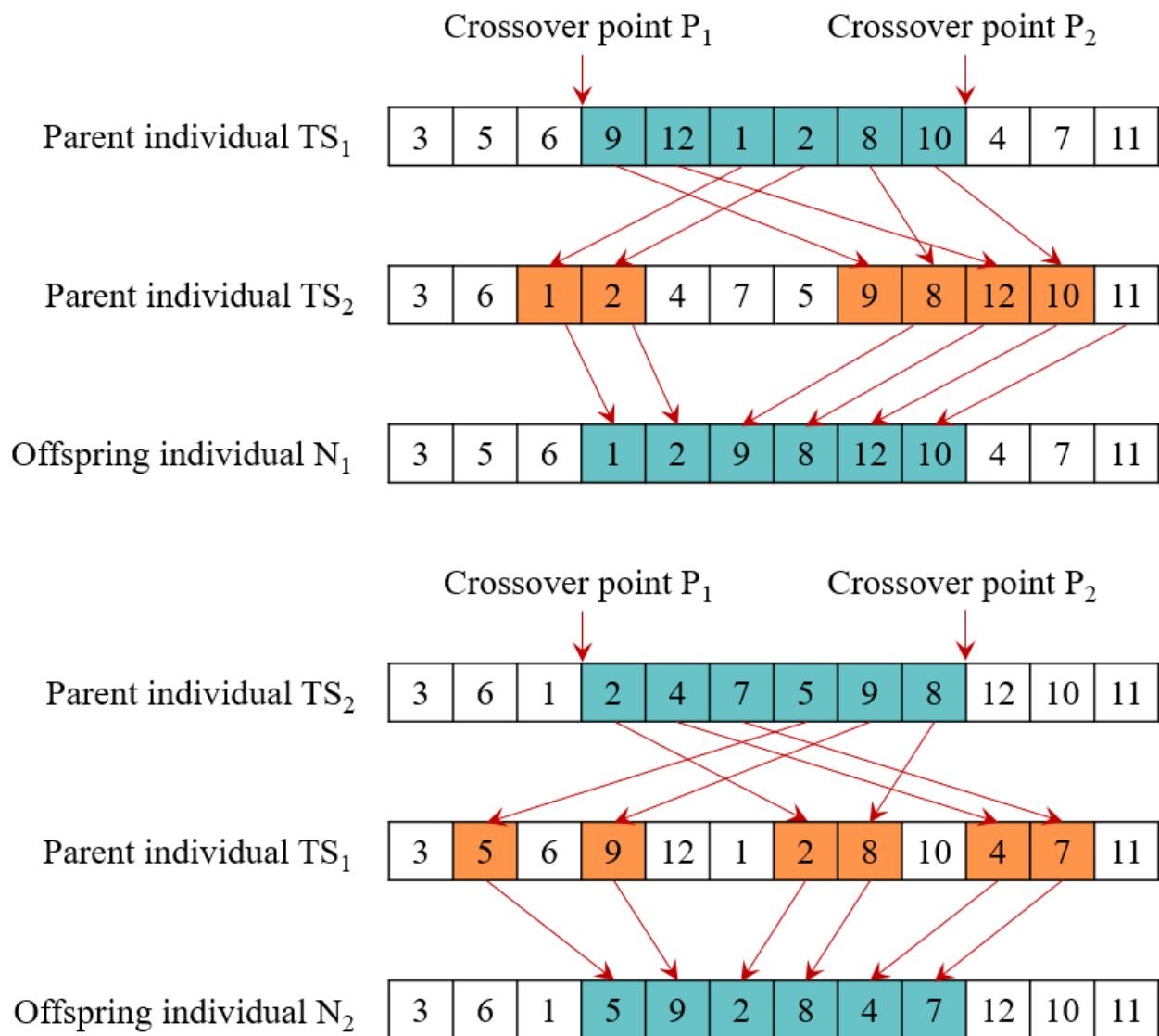


Figure 3. Individual crossover operation.

The crossover operation of the task decision vector and task mode vector is consistent with the crossover of the task sequence vectors. However, it should be noted that after the completion of the crossover of the task decision vector, the sequence should be checked and adjusted to ensure that the disassembly decision variable of all the predecessor tasks of the selected task is 1.

3.4. Mutation

A random mutation of the task sequence vector can also create infeasible individuals. A single-point mutation operator based on a precedence constraint is employed to find a feasible individual. The individual TS is regarded as the parent of the single-point mutation operation, as depicted in Figure 4. In TS, first a mutation point P is chosen at random, and the closest predecessor {3} and successor {8} tasks of the chosen task are identified. The chosen task {5} is then randomly inserted between the predecessor and successor to create the feasible individual set [33]. The offspring individual N {3, 5, 6, 1, 2, 4, 7, 9, 8, 12, 10, 11} is then chosen at random from the set.

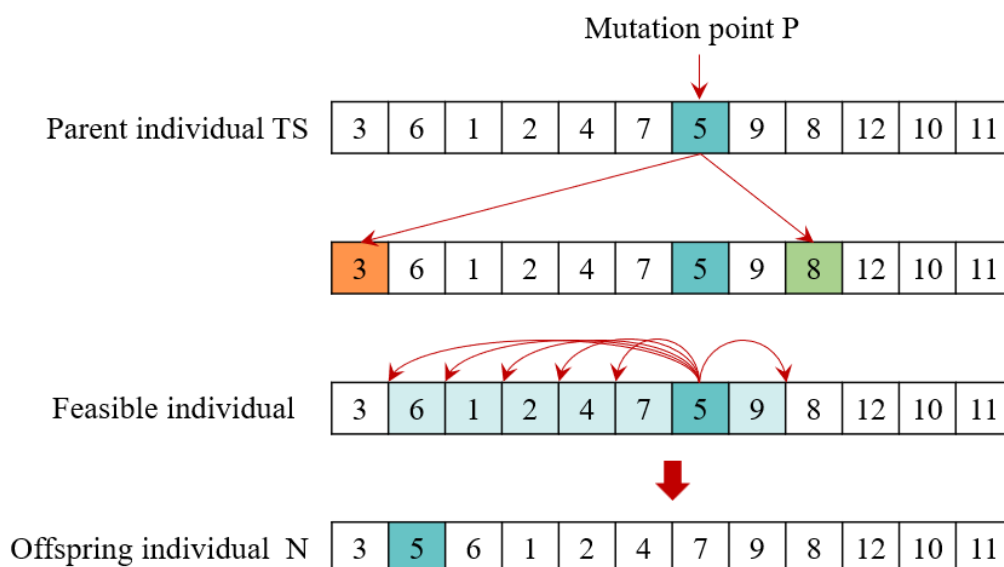


Figure 4. Individual mutation operation.

The task decision vector and task mode vector adopt the same mutation operation as the task sequence vector. Following the mutation of the task decision vector, the sequence should also be verified and corrected.

4. Case Study

A practical case of automobile is selected to verify the reliability and validity of the proposed model and method. Table 2 illustrates the 74 tasks that make up the entire process of disassembling an automobile. It includes information such as the hazardous property (h), the demanded property (d), the preferred operation direction (k), the disassembly mode ϵ , the disassembly time (t) for three models (m), the revenue (v), and the type of tools (o) of each task. Figure 5 depicts the relationships between tasks in terms of priority. The precedence relationship, the preferred operation direction, and hazardous property for each task are taken from Liang [15] et al. The population and iteration times of the algorithm are set as 100 and 500. The crossover probability and mutation probability involved in the algorithm are set as 0.8 and 0.2, respectively. Minimum product set is $MPS = \{1, 1, 1\}$.

Table 2. Tasks information of the automobile disassembly.

No.	Parts	h	d	k	$e = 1$					$e = 0$				
					t			v	o	t			v	o
					m_1	m_2	m_3			m_1	m_2	m_3		
1	Left engine hood hinge	0	0	L	20	18	17	19	6	2	2	2	14	9
2	Right engine hood hinge	0	0	R	17	21	13	19	1	2	2	2	14	9
3	Engine hood	0	1	E	10	15	12	833	6	1	2	1	625	9
4	Airbag	1	1	L	100	103	91	1296	6	9	9	8	972	7
5	Battery	1	0	R	33	39	39	110	5	3	4	4	83	8
6	Fuse Box	1	0	R	28	27	30	18	3	3	3	3	14	8
7	Waste fluid	1	0	E	13	8	16	20	6	2	1	2	15	7
8	Waste oil	1	0	E	195	202	143	2	3	17	17	12	2	7

Table 2. Cont.

No.	Parts	h	d	k	$e = 1$					$e = 0$				
					t		v	o		t		v	o	
					m_1	m_2	m_3	-	-	m_1	m_2	m_3	-	-
9	Refrigerant	1	0	E	63	38	43	17	4	6	4	4	13	8
10	Left front wheel	0	0	L	41	31	31	130	1	4	3	3	98	7
11	Left rear wheel	0	0	L	27	41	29	130	5	3	4	3	98	7
12	Right front wheel	0	0	R	32	22	30	130	4	3	2	3	98	8
13	Right rear wheel	0	0	R	38	40	39	130	3	4	4	4	98	9
14	Left fender	0	0	L	22	20	21	31	6	2	2	2	23	8
15	Right fender	0	0	R	22	33	24	31	5	2	3	2	23	8
16	Left front bumper	0	0	L	43	23	43	182	5	4	2	4	137	8
17	Right front bumper	0	0	R	23	38	42	182	2	2	4	4	137	8
18	Front bumper	0	0	E	17	19	14	285	5	2	2	2	214	7
19	Air intake grille	0	0	E	29	18	22	107	2	3	2	2	80	8
20	Left lamps	0	0	L	31	24	26	944	2	3	2	3	708	9
21	Right lamps	0	0	R	25	42	30	944	1	3	4	3	708	7
22	Left front door	0	1	L	38	44	44	1149	1	4	4	4	862	9
23	Left rear door	0	1	L	29	45	48	1149	3	3	4	4	862	8
24	Right front door	0	1	R	51	38	48	746	4	5	4	4	560	9
25	Right rear door	0	1	R	50	34	42	746	2	5	3	4	560	8
26	Left trunk cover hinge	0	0	L	19	19	17	61	3	2	2	2	46	8
27	Right trunk cover hinge	0	0	R	20	15	17	61	2	2	2	2	46	9
28	Trunk cover	0	1	E	41	27	22	910	1	4	3	2	683	7
29	Spare wheel	0	0	E	23	20	32	83	5	2	2	3	62	7
30	Left rear bumper	0	0	L	35	24	28	159	4	3	2	3	119	9
31	Right rear bumper	0	0	R	28	33	38	159	5	3	3	4	119	9
32	Rear bumper	0	0	E	13	19	14	244	1	2	2	2	183	8
33	Radiator	0	0	E	56	56	48	742	1	5	5	4	557	9
34	Condenser	0	0	E	48	62	77	409	1	4	6	7	307	9
35	Coolant tank	1	0	E	70	71	53	452	5	6	6	5	339	8
36	Air cleaner	0	0	E	38	35	28	787	5	4	3	3	590	7
37	Wiper	0	0	E	33	32	32	123	5	3	3	3	92	8
38	Wiper motor	0	0	E	37	30	26	58	4	4	3	3	44	8
39	Left front windscreen	0	0	L	42	56	52	70	4	4	5	5	53	7
30	Right front windscreen	0	0	R	57	43	42	70	4	5	4	4	53	7
41	Front windscreen	1	0	E	30	32	18	248	3	3	3	2	186	8
42	Left rear windscreen	0	0	L	23	33	25	51	3	2	3	3	38	9
43	Right rear windscreen	0	0	R	33	33	26	51	3	3	3	3	38	8
44	Rear windscreen	1	0	E	24	23	20	156	5	2	2	2	117	9
45	Left seat	0	1	L	95	126	100	977	3	8	11	9	733	7
46	Right seat	0	1	R	137	134	149	1186	6	12	12	13	890	9
47	Armrest box	0	0	E	37	68	35	25	5	4	6	3	19	9
48	Fuel tank	1	0	R	43	76	77	637	6	4	7	7	478	7
49	Steering wheel	0	0	L	56	39	47	189	2	5	4	4	142	9
50	Left center console bolt	0	0	L	63	67	59	1	2	6	6	5	1	9
51	Right center console bolt	0	0	R	50	36	46	2	2	5	3	4	2	8
52	Center console panel	0	0	E	38	34	44	438	3	4	3	4	329	8

Table 2. Cont.

No.	Parts	h	d	k	$e = 1$					$e = 0$				
					t			v	o	t			v	o
					m_1	m_2	m_3	-	-	m_1	m_2	m_3	-	-
53	Dashboard	0	0	L	48	39	35	508	3	4	4	3	381	7
54	Shift handle	0	0	E	68	76	60	106	6	6	7	5	80	9
55	Brake rigging	0	0	L	89	103	77	226	2	8	9	7	170	9
56	Clutch pedal	0	0	L	27	25	35	81	2	3	3	3	61	9
57	Accelerator pedal	0	0	L	39	36	39	81	6	4	3	4	61	8
58	Air conditioner	0	1	E	47	64	70	660	5	4	6	6	495	8
59	Steering system	0	0	L	103	121	121	512	4	9	11	11	384	8
60	Carbon canister	1	0	E	14	13	13	23	1	2	2	2	17	8
61	Bottom guard board	0	0	E	26	30	27	70	2	3	3	3	53	9
62	Exhaust pipe	1	1	E	70	41	53	1440	1	6	4	5	1080	9
63	Drive shaft	0	1	E	99	164	109	577	1	9	14	10	433	7
64	Electric generator	0	0	E	103	100	96	392	1	9	9	8	294	9
65	Front suspension	0	0	E	122	102	109	64	1	11	9	10	48	7
66	Rear suspension	0	0	E	93	116	128	57	6	8	10	11	43	8
67	Engine	0	1	E	163	180	213	6188	4	14	15	18	4641	8
68	Transmission	0	1	E	117	156	93	6562	2	10	13	8	4922	8
69	Left decoration	1	0	L	47	47	80	91	1	4	4	7	68	9
70	Right decoration	1	0	R	45	76	56	62	4	4	7	5	47	7
71	Interior light	1	0	E	24	16	19	8	4	2	2	2	6	9
72	Audio system	0	0	E	44	30	35	244	4	4	3	3	183	9
73	Left wiring harness	0	0	L	35	35	39	385	3	3	3	4	289	7
74	Right wiring harness	0	0	R	21	33	31	331	1	2	3	3	248	7

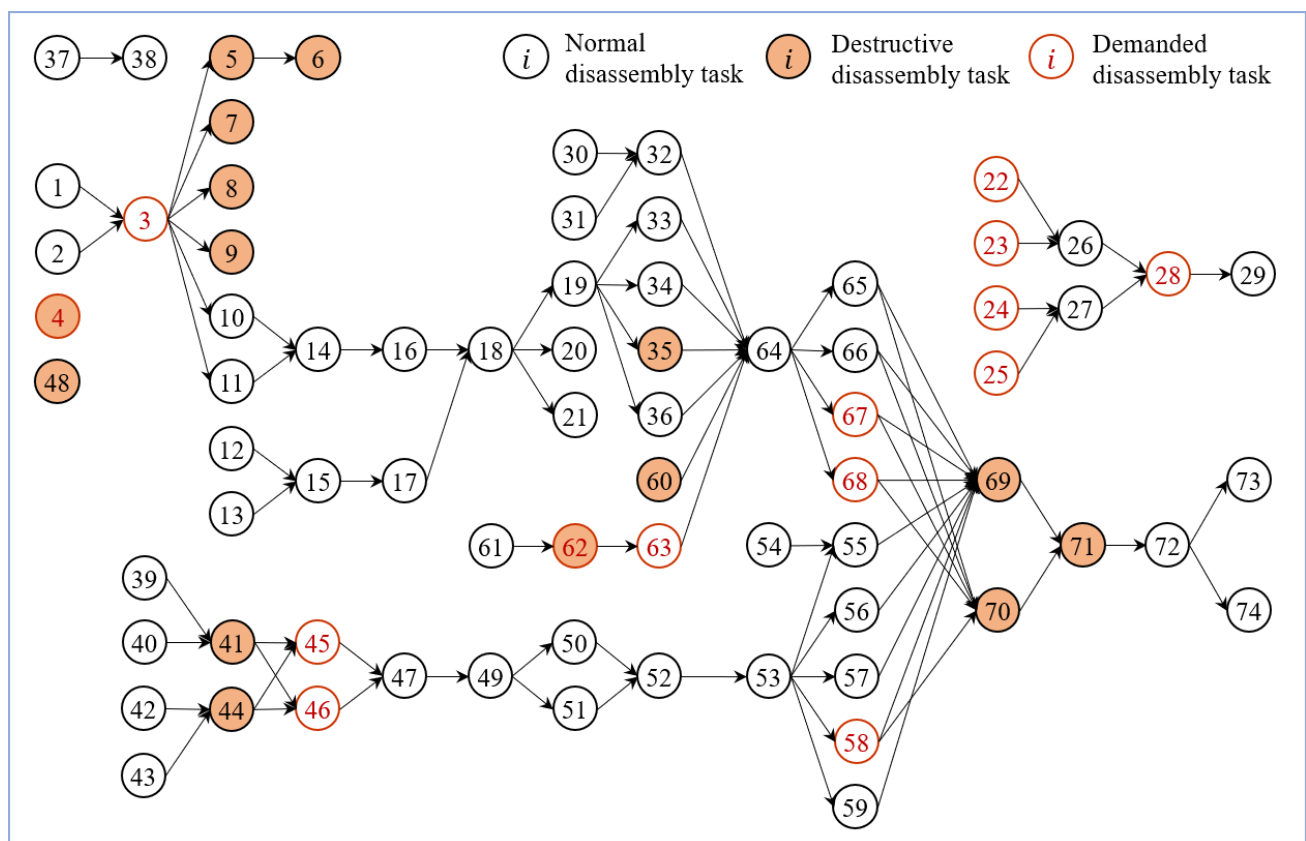


Figure 5. Precedence relationships among the parts of the waste automobile.

The cycle time of the disassembly line is 521 s. The conventional disassembly times of each model are randomly generated between $1/3 \sim 2/3$ of the original task times. The destructive disassembly times are achieved by multiplying the conventional disassembly times by $1/12$. The disassembly costs of different types of tools are shown in Table 3. The revenue generated from the conventional disassembly is randomly generated within the range of 20% to 50% of its market value. The revenue generated from the destructive disassembly is $3/4$ of that from a conventional disassembly. The other auxiliary parameters are as follows: $c_s = 1$ RMB/s, $c_h = 0.2$ RMB/s, $c_f = 200$ RMB, $t_t = 2$ s.

Table 3. Disassembly costs of different types of tools.

o	1	2	3	4	5	6	7	8	9
c	6	10	8	4	7	9	2	5	3

NSGA-II algorithm has been run 10 times and 12 Pareto solutions have been obtained. The Pareto front of the algorithm is shown in Figure 6. The three objective function values of the Pareto front corresponding to Figure 6 are shown in Table 4. It can be seen from the results of f_1 and f_2 that there is a trade-off between the number of workstations and profit. This may be related to the longer disassembly time of high-value parts. However, from the results of f_3 , there is no significant correlation between the smoothness index and the number of workstations or between the smoothness index and profit; this is because the station time varies between disassembly schemes. This is consistent with the conclusion of Wang [7] et al.

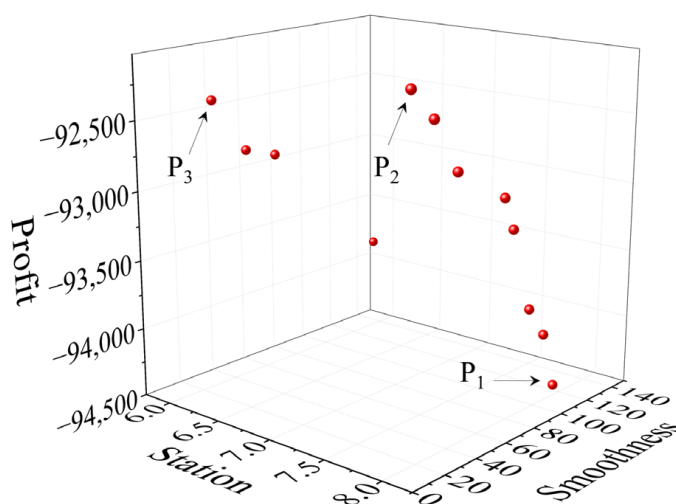


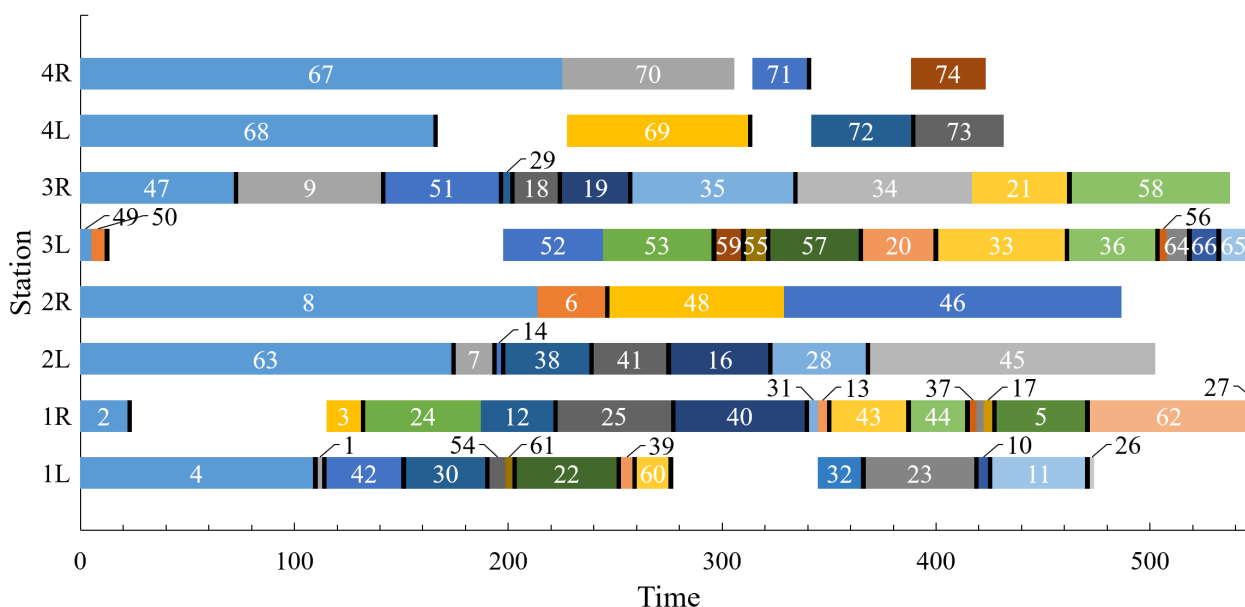
Figure 6. The Pareto front of NSGA-II.

In order to evaluate the benefits of the partial destructive mode, profits are calculated for each of the three modes (partial destructive mode, conventional mode, and destructive mode) as shown in Table 4. In the destructive mode, harmful parts and high-value parts are still disassembled in a conventional way, and the rest of the parts are disassembled destructively. The maximum values in the three results are highlighted in bold. It can be seen that in almost all results, the profit calculated under the partial destructive mode is the largest. The partial destructive mode clearly outperforms the conventional and destructive modes.

Table 4. The computational result of NSGA-II.

No.	f_1	f_2	$-f_3$		
			Partial Destructive Disassembly	Conventional Disassembly	Destructive Disassembly
1	6	67.4	−92,893.6	−91,939.6	−92,108.6
2	6	49.4	−92,807.6	−92,581.6	−92,126.6
3	6	29.6	−92,397.6	−92,581.6	−92,126.6
4	6	134.9	−93,804.6	−91,963.6	−92,084.6
5	8	15.9	−92,041.6	−91,939.6	−92,084.6
6	8	106.8	−94,004.6	−91,933.6	−92,072.6
7	8	44.9	−92,638.6	−91,945.6	−92,090.6
8	8	82.9	−93,152.6	−91,981.6	−92,090.6
9	8	95.7	−93,770.6	−92,557.6	−92,102.6
10	8	115.3	−94,423.6	−91,963.6	−92,126.6
11	8	29.8	−92,260.6	−91,969.6	−92,078.6
12	8	76.4	−92,911.6	−92,551.6	−92,102.6

The three points marked in Figure 6 correspond to schemes that obtain better value on each of the three objectives. These are point P_1 with the largest profit, point P_2 with the best smoothness, and point P_3 with the smallest workstation. The objective values (f_1 , f_2 , $-f_3$) of the three points are (8, 115.3, −94,423.6), (8, 15.9, −92,041.6), and (6, 29.6, −92,397.6), respectively. The Gantt charts corresponding to the three points are shown in Figures 7–9. It shows the task sequence, start, and end time of each task, and the tool changes between different tasks (filled with black in the figure). The disassembly scheme S_1 and S_2 are both performed on eight workstations. The optimal smoothness index can be obtained when scheme S_2 is adopted. A total of 19 tasks are destructively dismantled. Although it has minimal idle time, its profits are not the highest. When scheme S_1 is adopted, 22 tasks are destructively disassembled. The decrease in conventionally disassembled tasks, combined with the presence of the multi-constraint, resulted in a large amount of idle time, but it is still the most profitable scheme. In scheme S_3 , 31 tasks are destructively disassembled so that more tasks can be performed in fewer workstations. In this case, the impact on profit mainly comes from revenue of the parts and disassembly time cost, while the impact on profit from starting a new workstation is not the main one. Thus, there is a situation where six workstations have no advantage over eight workstations.

**Figure 7.** Gantt chart of disassembly scheme S_1 .

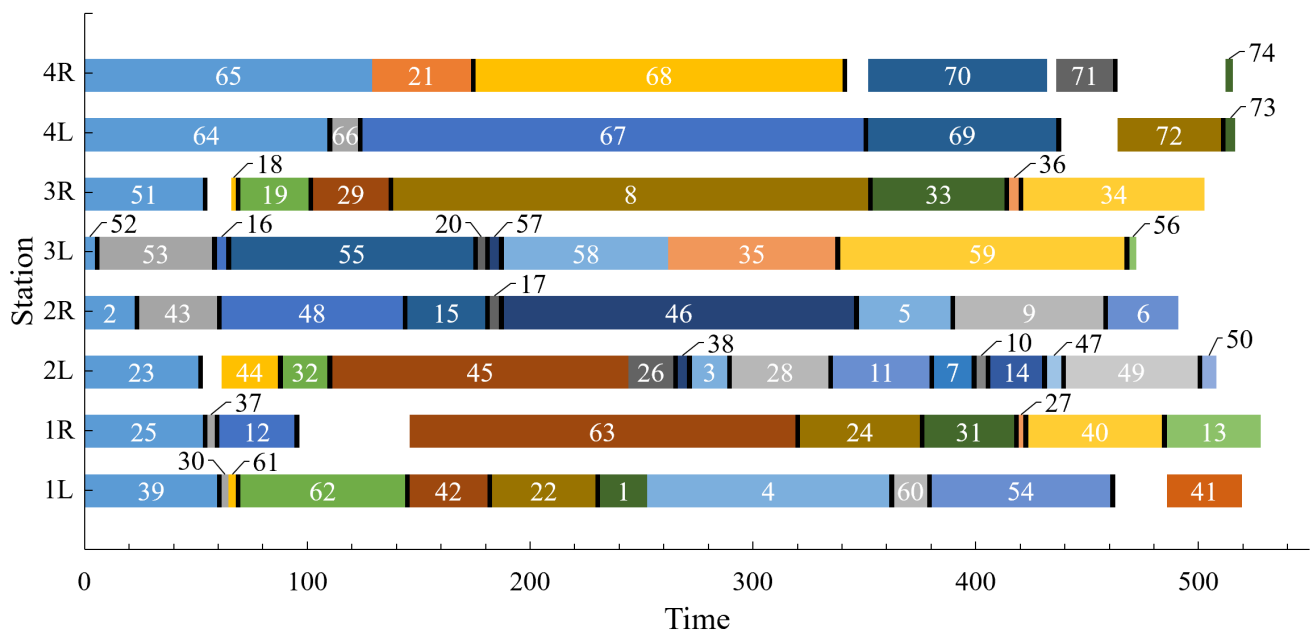


Figure 8. Gantt chart of disassembly scheme S_2 .

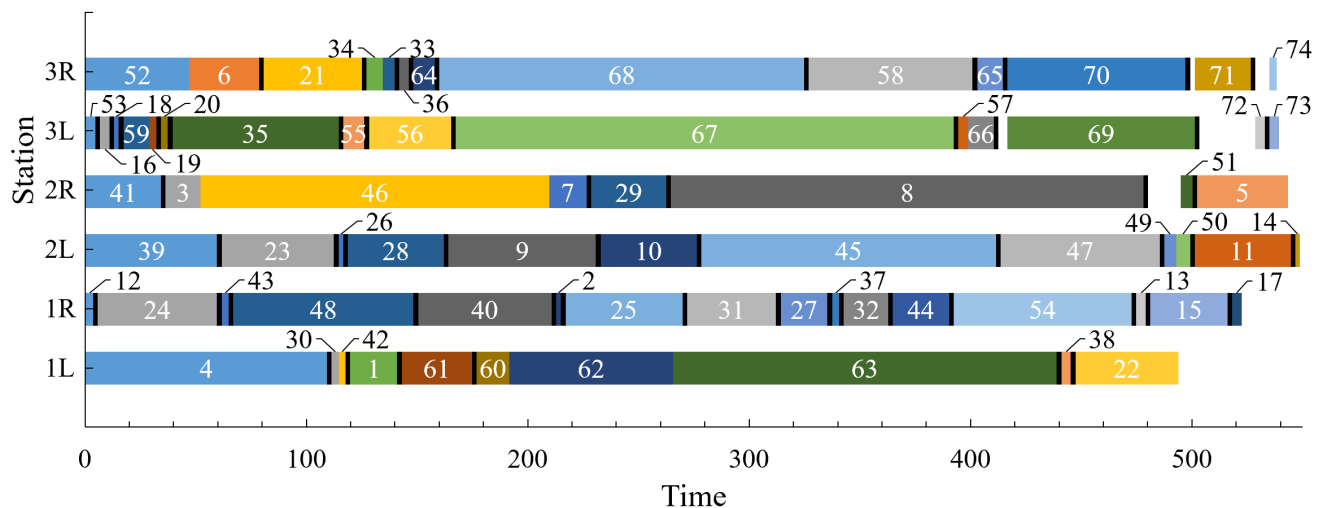


Figure 9. Gantt chart of disassembly scheme S_3 .

The disassembly scheme S_1 with the maximum profit is selected to analyse the relationships among task profit, revenue, and cost, as shown in Figure 10. Here, the cost is expressed as a negative value. As the disassembly operation progresses, the cost increases gradually. Although four new mated stations are opened, the cost does not change dramatically. This indicates that the cost is mainly the time cost of disassembly. The profit of disassembly increases with the increase in revenue. Among them, when the high-value parts corresponding to Task 67 (Engine) and Task 68 (Transmission) are disassembled, the revenue and profit are dramatically improved. This is due to a fact that the revenue of these two parts is much higher than their disassembly cost.

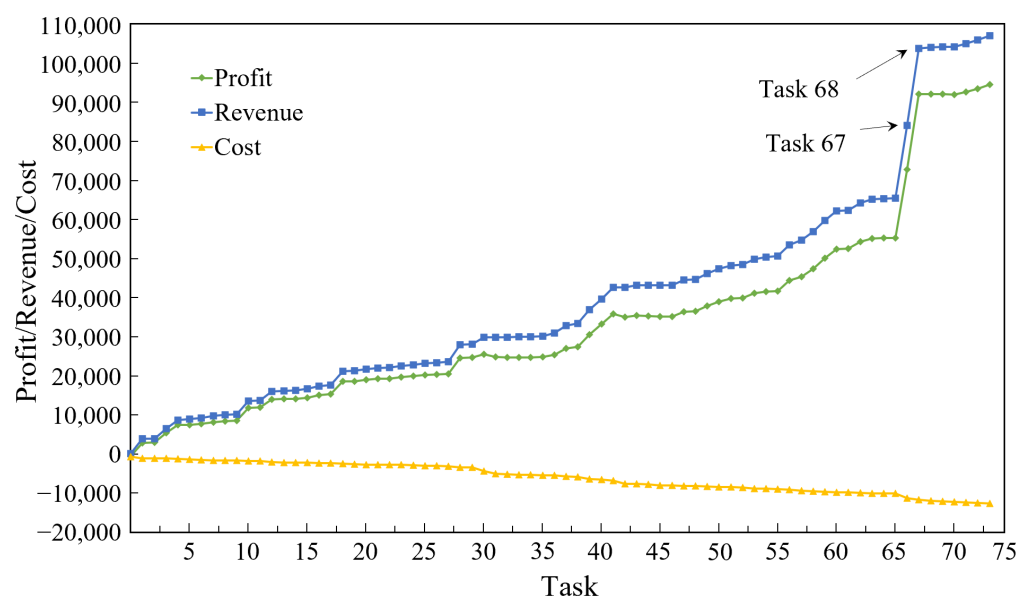


Figure 10. The relationships among task profit, revenue, and cost.

As can be seen from the above results, fewer workstations do not lead to higher profit. At the same time, better smoothness does not effectively increase profits. This is related to the characteristics of the partial destructive disassembly mode itself. When fewer workstations are pursued, more tasks may be destructively disassembled to assign more tasks in one workstation. When pursuing the best smoothness, high-value parts may be destructively disassembled in order to achieve the balance of tasks among workstations, thus they are unable to obtain higher benefits. For enterprises, profit is the first priority. When the factory site is sufficient, the disassembly scheme with a relatively large number of workstations but the highest profit should be selected.

5. Conclusions

This research innovatively designed a mixed-model two-sided disassembly line considering a partial destructive mode. Harmful parts and high-value parts are disassembled in a conventional mode, and other parts are disassembled randomly in a conventional or destructive mode. The impact of tool change on operation time is considered to more accurately describe the actual disassembly process. Then, the mathematical model of the disassembly process is established, and the three objectives of the number of workstations, the smoothness index, and the profit are optimized. In addition, in order to solve this combinatorial optimization problem efficiently, NSGA-II, which has been proved to be superior by many studies, is selected in this study, and the encoding, decoding, crossover, and mutation rules are redefined according to the characteristics of the problem. The results show that the partial destructive disassembly mode can maximize profits.

In this work, the mixed-model disassembly of large-volume products is studied from the perspective of a partial destructive mode, which provides a new research idea for the disassembly of waste products under uncertain conditions. The mathematical model and algorithm constructed in this paper can provide theoretical and technical guidance for the construction of large-volume products disassembly line.

Future research can be extended to many fields. This study did not take into account the correlation between parts. In the same disassembly sequence, whether the destructive disassembly of the predecessor will affect the disassembly mode of the successors is a problem worth further investigation. Further, disassembly lines for large-volume products can be combined with assembly lines for large-volume products, allowing economic and environmental indicators of the disassembly to assembly process to be considered at a more automated disassembly level.

Author Contributions: B.C.: Writing—Original draft, methodology. P.L.: software, data curation. C.Z.: validation, supervision. H.G.: validation. All authors have read and agreed to the published version of the manuscript.

Funding: This research was partially supported by the Project of International Cooperation and Exchanges NSFC [Grant No. 51861165202], the National Natural Science Foundation of China [Grant Nos. 51575211, 51705263, 51805330], the 111 Project of China [Grant No. B16019]. The authors thank the technical support from the Experiment Center for Advanced Manufacturing and Technology in the School of Mechanical Science & Engineering of HUST.

Data Availability Statement: The data that support the findings of this study are available from the corresponding author, upon reasonable request.

Conflicts of Interest: The authors declare no conflict of interest.

Appendix A

The parameters and variables required by the model are as follows:

- Indices:

i, j, a, b : Index of tasks, $i, j, a, b \in I$.

s, s' : Index of mated stations, $s, s' \in S$.

k : Side of the stations, left side, $k = 1$; right side, $k = 2$.

q : Position of the tasks within a workstation, $q \in Q$.

m : Product model, $m \in M$.

- Parameters:

I : Set of tasks, $I = \{1, 2, \dots, i, \dots, N_t\}$.

S : Set of mated stations, $S = \{1, 2, \dots, s, \dots, N_s\}$.

Q : Set of task positions, $Q = \{1, 2, \dots, q, \dots, N_q\}$.

M : Set of product model, $M = \{1, 2, \dots, m, \dots, N_m\}$.

t_{ie}^m : Disassembly time when the task i of model m adopts disassembly mode e .

t_t : Tool replacement time.

v_{ie} : Disassembly revenue when task i adopts disassembly mode e ;

c_{ie} : Disassembly cost when task i adopts disassembly mode e ;

c_s : Unit time cost of running the workstation.

c_h : The additional unit time cost to the workstation while handling hazardous tasks.

c_f : Fixed cost of starting workstation.

o_i : Type of tool for task i .

T_{sk} : Total disassembly time in workstation.

CT : Cycle time.

MPS : Minimum product set, $MPS = \{a_1, a_2, a_3, \dots, a_M\}$.

a_m : Number of models m in MPS , $a_m = A_m/L$, ($m = 1, 2, \dots, N_m$).

A_m : Number of products m .

L : The greatest common divisor of all A_m .

- Decision variables:

x_i : 1, if task i is performed, 0, otherwise.

x_{isk} : 1, if task i is assigned to the k side of the mated station s , 0, otherwise.

x_{iskq} : 1, if task i is assigned to position q on k side of the mated station s , 0, otherwise.

e_i : 1, if the task i is disassembled conventionally, 0, if the task i is disassembled destructively.

W_{sk} : 1, if the k side of the mated station s is used, 0, otherwise.

G_s : 1, if the entire mated station s is used, 0, otherwise.

F_s : 1, if only one side of the mated station s is used, 0, otherwise.

y_{ijs} : For mated station s , 1, if task i is assigned to the s before task j , 0, otherwise.

- Indicator variables:

h_i : 1, if the task i is hazardous, 0, otherwise.

d_i : 1, if the task i is demanded, 0, otherwise.

z_{ij} : 1, if the disassembly tools for task i and task j are different, 0, otherwise.

P_{ij} : 1, if task j is an immediate predecessor of task i , 0, otherwise.

References

1. Rehman, S.U.; Kraus, S.; Shah, S.A.; Khanin, D.; Mahto, R.V. Analyzing the relationship between green innovation and environmental performance in large manufacturing firms. *Technol. Forecast. Soc. Chang.* **2021**, *163*, 120481. [\[CrossRef\]](#)
2. Guo, H.F.; Lian, X.; Zhang, Y.; Ren, Y.P.; He, Z.B.; Zhang, R.; Ding, N. Analysis of Environmental Policy's Impact on Remanufacturing Decision Under the Effect of Green Network Using Differential Game Model. *IEEE Access* **2020**, *8*, 115251–115262. [\[CrossRef\]](#)
3. Wu, J.Z.; Lian, K.L.; Deng, Y.L.; Jiang, P.; Zhang, C.Y. Multi-Objective Parameter Optimization of Fiber Laser Welding Considering Energy Consumption and Bead Geometry. *IEEE Trans. Autom. Sci. Eng.* **2022**, *19*, 3561–3574. [\[CrossRef\]](#)
4. Wu, J.Z.; Zhang, C.Y.; Lian, K.L.; Cao, H.J.; Li, C.B. Carbon emission modeling and mechanical properties of laser, arc and laser-arc hybrid welded aluminum alloy joints. *J. Clean. Prod.* **2022**, *378*, 134437. [\[CrossRef\]](#)
5. Gungor, A.; Gupta, S.M.; Pochampally, K.; Kamarthi, S.V. Complications in disassembly line balancing. In Proceedings of the 1st International Conference on Environmentally Conscious Manufacturing, Boston, MA, USA, 6–8 November 2000; pp. 289–298.
6. Wu, K.; Guo, X.W.; Liu, S.X.; Qi, L.; Zhao, J.; Zhao, Z.Y.; Wang, X. IEEE Multi-objective Discrete Brainstorming Optimizer for Multiple-product Partial U-shaped Disassembly Line Balancing Problem. In Proceedings of the 33rd Chinese Control and Decision Conference (CCDC), Kunming, China, 22–24 May 2021; pp. 305–310.
7. Wang, K.P.; Li, X.Y.; Gao, L.; Li, P.G. Energy consumption and profit-oriented disassembly line balancing for waste electrical and electronic equipment. *J. Clean. Prod.* **2020**, *265*, 121829. [\[CrossRef\]](#)
8. Paprocka, I.; Skolud, B. A Predictive Approach for Disassembly Line Balancing Problems. *Sensors* **2022**, *22*, 3920. [\[CrossRef\]](#)
9. Wu, T.F.; Zhang, Z.Q.; Yin, T.; Zhang, Y. Multi-objective optimisation for cell-level disassembly of waste power battery modules in human-machine hybrid mode. *Waste Manag.* **2022**, *144*, 513–526. [\[CrossRef\]](#)
10. Ren, Y.P.; Zhang, C.Y.; Zhao, F.; Triebe, M.J.; Meng, L.L. An MCDM-Based Multiobjective General Variable Neighborhood Search Approach for Disassembly Line Balancing Problem. *IEEE Trans. Syst. Man Cybern. Syst.* **2020**, *50*, 3770–3783. [\[CrossRef\]](#)
11. Liang, W.; Zhang, Z.Q.; Zhang, Y.; Xu, P.Y.; Yin, T. Improved social spider algorithm for partial disassembly line balancing problem considering the energy consumption involved in tool switching. *Int. J. Prod. Res.* **2022**, 1–17. [\[CrossRef\]](#)
12. Guo, H.F.; Zhang, L.S.; Ren, Y.P.; Li, Y.; Zhou, Z.W.; Wu, J.Z. Optimizing a stochastic disassembly line balancing problem with task failure via a hybrid variable neighborhood descent-artificial bee colony algorithm. *Int. J. Prod. Res.* **2022**, 1–15. [\[CrossRef\]](#)
13. Bentaha, M.L.; Marange, P.; Voisin, A.; Moalla, N. End-of-Life product quality management for efficient design of disassembly lines under uncertainty. *Int. J. Prod. Res.* **2022**, 1–22. [\[CrossRef\]](#)
14. Paksoy, T.; Gungor, A.; Ozceylan, E.; Hancilar, A. Mixed model disassembly line balancing problem with fuzzy goals. *Int. J. Prod. Res.* **2013**, *51*, 6082–6096. [\[CrossRef\]](#)
15. Liang, J.Y.; Guo, S.S.; Xu, W.X. Balancing Stochastic Mixed-Model Two-Sided Disassembly Line Using Multiobjective Genetic Flatworm Algorithm. *IEEE Access* **2021**, *9*, 138067–138081. [\[CrossRef\]](#)
16. McGovern, S.M.; Gupta, S.M. Combinatorial optimization analysis of the unary NP-complete disassembly line balancing problem. *Int. J. Prod. Res.* **2007**, *45*, 4485–4511. [\[CrossRef\]](#)
17. Lambert, A.J.D. Linear programming in disassembly/clustering sequence generation. *Comput. Ind. Eng.* **1999**, *36*, 723–738. [\[CrossRef\]](#)
18. Bentaha, M.L.; Battaia, O.; Dolgui, A. An exact solution approach for disassembly line balancing problem under uncertainty of the task processing times. *Int. J. Prod. Res.* **2015**, *53*, 1807–1818. [\[CrossRef\]](#)
19. Ren, Y.P.; Meng, L.L.; Zhao, F.; Zhang, C.Y.; Guo, H.F.; Tian, Y.; Tong, W.; Sutherland, J.W. An improved general variable neighborhood search for a static bike-sharing rebalancing problem considering the depot inventory. *Expert Syst. Appl.* **2020**, *160*, 113752. [\[CrossRef\]](#)
20. Avikal, S.; Mishra, P.K.; Jain, R. A Fuzzy AHP and PROMETHEE method-based heuristic for disassembly line balancing problems. *Int. J. Prod. Res.* **2014**, *52*, 1306–1317. [\[CrossRef\]](#)
21. McGovern, S.M.; Gupta, S.M. 2-opt heuristic for the disassembly line balancing problem. In Proceedings of the 3rd International Conference on Environmentally Conscious Manufacturing, Providence, RI, USA, 29–30 October 2003; pp. 71–84.
22. Cheng, C.Y.; Chen, Y.Y.; Pourhejazy, P.; Lee, C.Y. Disassembly Line Balancing of Electronic Waste Considering the Degree of Task Correlation. *Electronics* **2022**, *11*, 533. [\[CrossRef\]](#)
23. Kizilay, D. A novel constraint programming and simulated annealing for disassembly line balancing problem with AND/OR precedence and sequence dependent setup times. *Comput. Oper. Res.* **2022**, *146*, 105915. [\[CrossRef\]](#)
24. Cil, Z.A.; Mete, S.; Serin, F. Robotic disassembly line balancing problem: A mathematical model and ant colony optimization approach. *Appl. Math. Model.* **2020**, *86*, 335–348. [\[CrossRef\]](#)
25. Ren, Y.P.; Yu, D.Y.; Zhang, C.Y.; Tian, G.D.; Meng, L.L.; Zhou, X.Q. An improved gravitational search algorithm for profit-oriented partial disassembly line balancing problem. *Int. J. Prod. Res.* **2017**, *55*, 7302–7316. [\[CrossRef\]](#)
26. Guo, X.W.; Zhang, Z.W.; Qi, L.; Liu, S.X.; Tang, Y.; Zhao, Z.Y. Stochastic Hybrid Discrete Grey Wolf Optimizer for Multi-Objective Disassembly Sequencing and Line Balancing Planning in Disassembling Multiple Products. *IEEE Trans. Autom. Sci. Eng.* **2022**, *19*, 1744–1756. [\[CrossRef\]](#)
27. Lu, Q.; Ren, Y.P.; Jin, H.Y.; Meng, L.L.; Li, L.; Zhang, C.Y.; Sutherland, J.W. A hybrid metaheuristic algorithm for a profit-oriented and energy-efficient disassembly sequencing problem. *Robot. Comput. Integr. Manuf.* **2020**, *61*, 101828. [\[CrossRef\]](#)

28. Kucukkoc, I. Balancing of two-sided disassembly lines: Problem definition, MILP model and genetic algorithm approach. *Comput. Oper. Res.* **2020**, *124*, 105064. [[CrossRef](#)]
29. Macaskill, J. Production-line balances for mixed-model lines. *Manag. Sci.* **1972**, *19*, 423–434. [[CrossRef](#)]
30. Wang, K.; Li, X.; Gao, L.; Li, P.; Sutherland, J.W. A Discrete Artificial Bee Colony Algorithm for Multiobjective Disassembly Line Balancing of End-of-Life Products. *IEEE Trans. Cybern.* **2022**, *52*, 7415–7426. [[CrossRef](#)]
31. Delice, Y.; Aydogan, E.K.; Ozcan, U.; Ilkay, M.S. A modified particle swarm optimization algorithm to mixed-model two-sided assembly line balancing. *J. Intell. Manuf.* **2017**, *28*, 23–36. [[CrossRef](#)]
32. Tian, G.; Zhang, C.; Fathollahi-Fard, A.M.; Li, Z.; Zhang, C.; Jiang, Z. An Enhanced Social Engineering Optimizer for Solving an Energy-Efficient Disassembly Line Balancing Problem Based on Bucket Brigades and Cloud Theory. *IEEE Trans. Ind. Inform.* **2022**, *1*–11. [[CrossRef](#)]
33. Tian, G.D.; Yuan, G.; Aleksandrov, A.; Zhang, T.Z.; Li, Z.W.; Fathollahi-Fard, A.M.; Ivanov, M. Recycling of spent Lithium-ion Batteries: A comprehensive review for identification of main challenges and future research trends. *Sustain. Energy Technol. Assess.* **2022**, *53*, 102447. [[CrossRef](#)]

Disclaimer/Publisher’s Note: The statements, opinions and data contained in all publications are solely those of the individual author(s) and contributor(s) and not of MDPI and/or the editor(s). MDPI and/or the editor(s) disclaim responsibility for any injury to people or property resulting from any ideas, methods, instructions or products referred to in the content.